Attributing Venice Acqua Alta events to a changing climate and evaluating the efficacy of MoSE adaptation strategy

Davide Faranda, Mireia Ginesta, Tommaso Alberti, Erika Coppola, Marco Anzidei

Attributing Venice Acqua Alta events to a changing climate and evaluating the efficacy of MoSE adaptation strategy

Davide Faranda[1,2,3*], Tommaso Alberti[4], Erika Coppola[5], Marco Anzidei[4]

[1*]Laboratoire des Sciences du Climat et de l'Environnement, CEA Saclay l'Orme des Merisiers, UMR 8212 CEA-CNRS-UVSQ, Gif-sur-Yvette, 91191, France.
[2]London Mathematical Laboratory, 8 Margravine Gardens, London, W6 8RH, UK.
[3]Laboratoire de Météorologie Dynamique/IPSL, École Normale Supérieure, PSL Research University, Sorbonne Université, 75005, Paris, France, École Polytechnique, IP Paris, Paris, 75005, France.
[4]Istituto Nazionale di Geofisica e Vulcanologia, via di Vigna Murata 605, Rome, 00143, Italy.
[5]International Centre for Theoretical Physics, Strada Costiera 11, Trieste, 34100, Italy.

*Corresponding author(s). E-mail(s): davide.faranda@lsce.ipsl.fr;
Contributing authors: tommaso.alberti@ingv.it; coppolae@ictp.it; marco.anzidei@ingv.it;

Abstract

We use analogues of atmospheric patterns to investigate changes in the three most devastating Acqua Alta (flooding) events in the lagoon of Venice associated with intense Mediterranean cyclones occurred in 1966, 2018 and 2019. Our results provide evidence that changes in atmospheric circulation, although not necessarily anthropogenically driven only, are linked to the severity of these events. We also evaluate the cost and benefit of the MoSE system, which was designed to protect against flooding. Our analysis shows that the MoSE has already provided protection against analogues of the most extreme events, which occurred in 1966, while for 2018 and 2019 events our analysis is non-conclusive because of the lack

of analogues situations of those events. These findings have significant implications for the future of Venice and other coastal cities facing similar challenges from rising sea levels due to extreme events. This study also provide a pathway to evaluate the effectiveness of adaptation in a scenario more frequent and intense extreme events if higher global warming levels will be reached.

Keywords: Climate Change, Attribution, Sea Level, Adaptation, Mitigation

The Acqua Alta events in Venice have caused significant damage to the cultural and economic heritage of the city over the years [1]. These events, which involve the flooding of the city's streets and buildings, have become increasingly frequent and severe in recent decades [2, 3]. The three most devastating Acqua Alta events in the lagoon, which occurred on 04/11/1966, 29/10/2018, and 12/11/2019, have particularly impacted the city's cultural and economic heritage [4]. The 1966 event, also known as the "Great Flood of Venice", caused widespread damage to buildings and artworks, including the historic St. Mark's Basilica. The 2018 and 2019 events, which occurred within a year of each other, caused significant damage to the city's cultural landmarks and businesses, including the iconic Caffè Florian and many of the city's historic shops [5]. Figure 1 provides a schematic representation of the hazards faced by the Venice lagoon due to rising sea levels. It shows the relationship between sea level, flooded area, and estimated damages. An empirical approach has been used to estimate the relation between the sea level reached within the lagoon and the economic damages based on data available for the three devastating events. An analytical function was found using an exponential law to link economic damage and observed sea level change. The parameters of the fit were estimated using the Levenberg-Marquardt algorithm and assessed for robustness using the Least Absolute Residuals method (see Methods). The Figure also highlights significant flooding levels, such as the level at which foodbridges are needed to walk across St. Mark's square and the level at which water enters the St. Mark's Basilica.

Acqua Alta events in Venice are primarily caused by a combination of two main factors: the tides and the synoptic weather conditions. The high tides are a natural occurrence that are affected by the position and phases of the moon and other celestial bodies. However, when strong winds blow across the Adriatic Sea towards the Venetian Lagoon, they can cause an increase in the water level, known as storm surge. This is because the winds push the water towards the city and the narrow entrance of the lagoon limits its ability to escape. When this storm surge coincides with high tides, it can result in Acqua Alta events, where the water level rises above the level of the city's streets and floods the low-lying areas. The synoptic weather situation that causes these strong winds is typically a low-pressure system over the Tyrrhenian Sea (Genoa Low) combined with high-pressure systems over central and northern Europe, creating a strong pressure gradient and thus strong winds blowing towards Venice, causing potentially hazardous conditions. The impacts of the Genoa Low system as well as Mediterranean cyclones have been widely documented in literature [6–10],

emphasizing the importance of understanding this synoptic weather pattern in leading extreme events [11, 12].

Climate change is widely considered to be a major contributing factor to the increased frequency and severity of extreme weather events, including storm surges and flooding [13]. The Intergovernmental Panel on Climate Change (IPCC) has stated that the increasing frequency and severity of extreme weather events are very likely caused by human activities, including the burning of fossil fuels and the resultant emissions of greenhouse gases. These activities have led to changes in the Earth's climate, which have in turn altered storm patterns, increased sea levels, and caused more frequent and severe weather events. Coastal zones, such as the historical city of Venice and its lagoon in the Northern Adriatic Sea, are particularly vulnerable to extreme sea levels, requiring a realistic approach to assess the risks and future projections of flooding, claiming for attribution studies of extreme weather events to climate change [14–19].

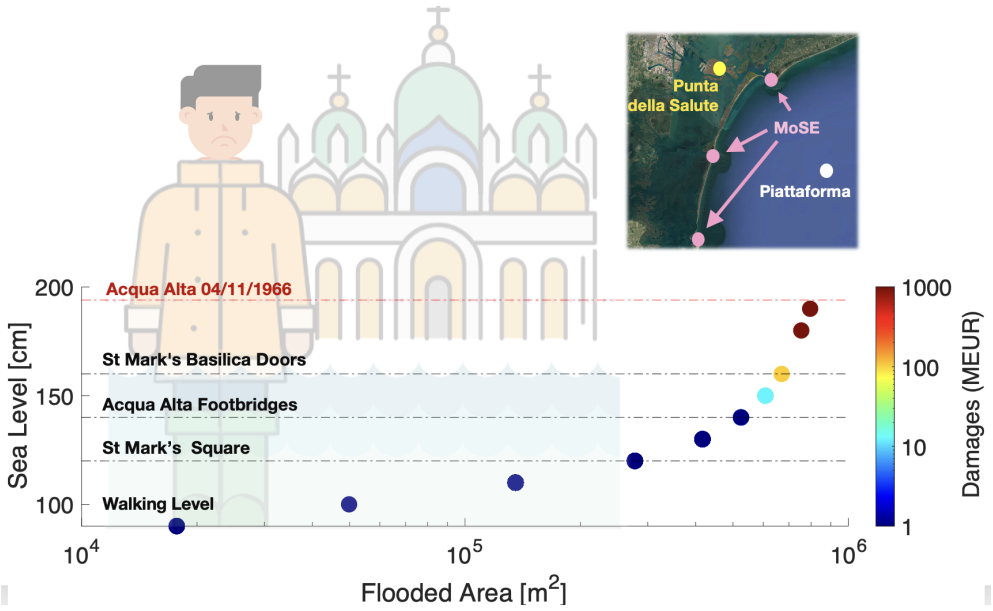

Fig. 1 Schematic representation of hazards for Venice lagoon. The relation between the sea level and the flooded area as a function of the estimated damages (filled colored circles). The horizontal dashed-dotted black lines mark significant flooding levels corresponding to the sea level flooding St. Mark's square (120 cm), the level at which foodbridges are needed to walk across the square (140 cm), and the level at which water will enter the St. Mark's Basilica (160 cm). The red dashed-dotted line marks the level reached by the 04/11/1966 event known as "Great Flood of Venice" and studied in this work. The inset shows the location of the two tide gauge stations used to evaluate the sea levels within the lagoon (Punta della Salute, yellow circle) and outside (Piattaforma, white circle). The pink circles mark instead the position of the MoSE barriers at the three inlets (Diga Nord, Malamocco, and Diga Sud). Adapted from https://www.comune.venezia.it/it/content/venezia-e-lacqua-alta.

Given the peculiarity the landscape, Venice is expected to be particularly vulnerable to climate change. Sea levels in Venice have risen by approximately 26 centimeters over the past century, with projections indicating a change in extreme total water level between 20 and 40 cm for RCP4.5 (2100) and RCP8.5 (2050) and up to 80 cm for the RPC8.5 (2100) [20]. Nevertheless, the complexity of the climate system and the challenges of climate change make difficult to evaluate the role of synoptic pattern changes in leading to Acqua Alta events [2, 4]. In the context of coastal floods in the city of Venice, there is a notable lack of studies that have attempted to attribute changes in atmospheric circulation over the Mediterranean region to specific causes. While there has been some research on the topic, the complex and dynamic nature of the Mediterranean climate system in relation to Venice, which is influenced by a range of factors including local topography, ocean currents, and large-scale weather patterns, presents significant challenges in identifying and understanding the underlying mechanisms driving changes in atmospheric circulation. Despite the limited research in this area, it is widely acknowledged that changes in atmospheric circulation patterns can have significant impacts on the frequency and intensity of coastal floods in Venice, as well as on the city's infrastructure and economy [21].

Despite these difficulties, the Italian government has invested about 6.2 billion euros in the Experimental Electromechanical Module (MoSE) project, which includes a series of mobile barriers located in the three main channels that connect the lagoon with the north Adriatic Sea [22–24]. The MoSE project has faced some delays and controversies, but the barriers were successfully tested in 2020 and are expected to become fully operational soon. However, the issue of Acqua Alta in Venice is complex and multifaceted, requiring a coordinated and sustained effort to address. The MoSE project represents an important step forward, but further action is needed to mitigate the impacts of climate change and protect this unique and valuable cultural heritage site. The inset in Figure 1 shows the location of the two tide gauge stations used to evaluate sea levels in this article (Punta della Salute and Piattaforma), while the pink circles indicate the position of the MoSE barriers at the three inlets.

In this paper, we employ a methodology that combines the use of analogue atmospheric patterns and statistical analysis [e.g., 25] to attribute the increasing frequency and severity of Acqua Alta events in Venice to climate change. Specifically, we use atmospheric circulation patterns from the three most devastating Acqua Alta events in the lagoon (04/11/1966 - 194 cm; 29/10/2018 - 156 cm; and 12/11/2019 - 187 cm) to identify analogues of these patterns in the recent past. By comparing the frequency of these analogues to the historical record, we assess the likelihood that the observed increase in Acqua Alta events is due to natural variability or climate change. To evaluate the effectiveness of MoSE (Experimental Electromechanical Module) protection, we analyze the analogues of the most extreme events and estimate the potential flood damage that would have occurred without MoSE activation. Finally, we perform a cost-benefit analysis to evaluate the economic implications of MoSE activation during Acqua Alta events.

Results

We compare the sea level pressure fields during Acqua Alta events in Venice from 1993-2022 to pressure from 1950-1979, when climate change was just beginning. The choice of the variable is justified by the need of reflecting the large-scale airflows that can drive extreme events such as floods. The method (see details below) ensures that comparisons are relevant, unlike purely statistical modeling techniques, which aim to simply analyze meteorological variables without tracing them back to the phenomena that produce them.

On November 4th, 1966, Venice experienced the highest Acqua Alta ever recorded since systematic measurements began. This was due to strong sirocco winds, a strong depression, and a disastrous storm surge that breached the Murazzi (a hydraulic defense structure) in multiple locations. The high water persisted for 22 hours above 110 cm and about 40 hours above 50 cm, causing significant damage to the city, including power and gas outages, flooded streets and buildings, and destroyed boats and businesses. The island of Sant'Erasmo disappeared under waves up to 4 meters high, and Murano's glass factories were almost entirely destroyed (https://nuovavenezia.gelocal.it/venezia/cronaca/2016/10/17/news/la-cronaca-dell-aqua-granda-a-venezia-4-novembre-1966-1.14265973).

The meteorological contribution to the Acqua Alta was impressive, reaching 185 cm, while the maximum coincided with an astronomical tide of only 9 cm. The sirocco winds prevented the outflow of water from the lagoon to the sea, and the minimum subsequent high tide was 116 cm. At 6:00 pm, the tide gauge at Punta della Salute reached 194 cm, the highest value ever recorded. Although other Italian cities were also severely affected by the storm, Venice was one of the most severely affected, and the city remained isolated for days. The slow recovery was carried out physically by the workers and technicians of ENEL as the power outages also had almost analogous effects on the phone lines.

Figure 2 displays the results of the attribution analysis for the 1966 Acqua Alta event in Venice. The study used the sea level pressure (SLP) field of the event (Figure 2a) to search for analogues for both counterfactual (Figure 2b) and factual (Figure 2c) periods in the domain 3°W-22°W 34°N-49°N. The SLP field of the event consists of a deep Genoa Low depression. The analysis found that the SLP field did not differ significantly between the two periods (Figure 2d) as well as temperature field (Figure 2e-h). The atmospheric pattern of the factual period is associated with higher precipitation over Lombardy, Veneto and Friuli which can enhance the contribution to Acqua Alta coming from the Adige and the Po Rivers (Figure 2i-l). Winds were generally stronger on the coasts of Provence and the Tyrrhenian coasts of central Italy, potentially contributing to orographic effects and increasing the amount of precipitation over the Alps, but not producing any significant changes in the Adriatic (Figure 2m-p).

The Supplementary Information and Figure S1 describe the diagnostic of the analogues analysis and the influence of interannual and interdecadal variability and shows that the event is exceptional in both periods analysed. These analyses also show that significant differences in the Pacific Decadal Oscillation (PDO) and Atlantic Multidecadal Oscillation (AMO) indices during the analogs day of the events are found

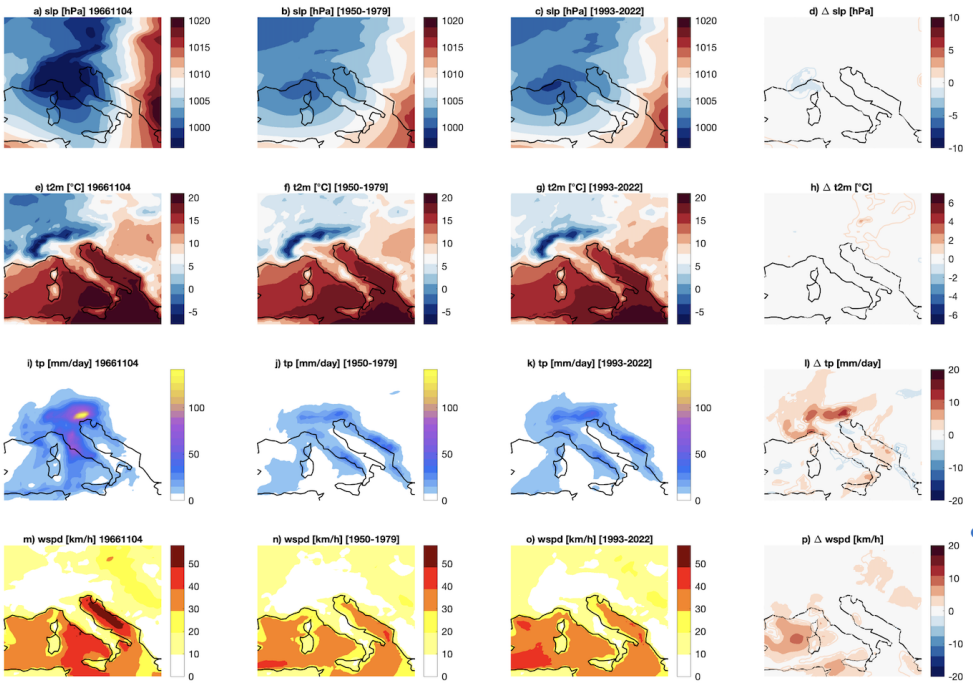

Fig. 2 Analogues Analysis for the 1966 Acqua Alta event in Venice. Daily mean sea-level pressure slp (a), 2-meter temperatures t2m (e), total precipitation tp (i), wind-speed wspd (m) on the day of the event. Average of the 17 sea-level pressure analogues found for the counterfactual [1950-1979] (b) and factual [1993-2022] (c) periods and corresponding 2-meter temperatures (f,g), daily precipitation rate (j,k) and wind speed (n,o). Δslp (d), Δt2m (h), Δtp (i) and Δwspd (p) between factual and counterfactual periods: colored-filled areas show significant anomalies with respect to the bootstrap procedure.

so that we cannot exclude a role of interdecadal variability in the changes of patterns identified in Figure 2. Figure S2-S3 shows the analysis for the 29/10/2018 and 12/11/2019 events respectively. While the 2018 event large scale circulation closely resembles that of the 1966 events but with a weaker depression, the 2019 event is associated with a cyclone that propagates from Liguria to the southern Tyrrhenian sea but the Acqua Alta was reinforced by a secondary depression on the Adriatic sea causing sudden changes of winds. Therefore, while the results of the analysis for the 2018 event (Figure S2) are similar to the ones described for the 1966 but with a less intense depression, for the 2019 event, we find that the event is unprecedented and no good-analogues can be found (Figure S3). Similarly to the 1966 event, for both 2018 and 2019 events, we cannot exclude a role of interannual and interdecadal variability in the changes associated with synoptic patterns leading to Acqua Alta events.

We now analyze the relationship between sea level (SL) and damages and evaluate whether the MoSE (Modulo Sperimentale Elettromeccanico) is effective in reducing the damages caused by Acqua Alta events in Venice that are similar (analogous) to the

	# MoSE	Variables	Event	[1950-1979]	[1993-2022]	[1993-2022] no MoSE
04/11/1966	5 (30%)	SL [cm]	194	123 [116, 194]	115 [69, 150]*	122 [111 150]
		Damages [MEUR]	8000	0.3 [0.1, 4000]	0.25 [0.01, 19]*	0.29 [0.07 19]
29/10/2018	1 (6%)	SL [cm]	156	122 [118,144]	125 [96, 155]	125 [111, 155]
		Damages [MEUR]	47	0.3 [0.2, 5.6]	0.5 [0.07, 26]	0.5 [0.07, 26]
12/11/2019	3 (20%)	SL [cm]	187	113 [113 114]	112 [62 183]	118 [110 183]
		Damages [MEUR]	1000	0.09 [0.09 1000]	0.2 [0.06 1600]	0.3 [0.06 1600]

Table 1 The table shows a summary of sea-levels (SL [cm]) and damages [MEUR] during the three largest Acqua alta historical events in Venice. # Mose indicates the number as well as the percentage of MoSE activations during the days anaologues of each event in the present period, the estimation of changes for SL and damages (median values and 5,95 percentiles of the analogues distributions in square brackets) for [1950-1979], [1993-2022] with MoSE activation (factual present) and [1993-2022] period where we assume that the MoSE was not activated (counterfactual present). '*' indicates significant changes with respect to the past period, determined used a Cramer von Mises test at 0.05 significance level [26].

worst three observed. Using the measurements available at both Punta della Salute and Piattaforma, we can construct two different statistics of SL and damages with factual [1993-2022] Punta della Salute MoSE values and a counterfactual present periods where Piattaforma values are used instead of Punta della Salute, and potential damages are estimated using the exponential model. For the statistics with the MoSE activated, we substitute the damages with the daily operational cost of the MoSE, estimated at 0.025 MEUR (https://www.pagellapolitica.it/articoli/costo-mose-venezia). This analysis allows us to evaluate whether the MoSE has already functioned as an effective mitigation strategy. Results of this analysis are reported in Table 1 and details on the distribution in Figures S1 for all events. First of all, we remark that the SL and the damages estimated during the three events are larger both of the median values and even of the 95% percentiles of the SL and the damages distribution. For the 1966 event, we find 5 analogues in the present periods that have activated the MoSE. When we compare both present factual and counterfactual periods with the past for the 1966 event, we notice a reduction of maximum damages, which is statistically significant when comparing the factual present with the past. For the 2018 event, there is only one analogue situation in the present period where MoSE has been activated. Therefore the cost of the MoSE activation is equivalent to the estimated damages. Finally, MoSE has been activated in three analogue situations of the 2019 event. The damages in the factual present appears to be higher compared to the past, but still lower when compared to the counterfactual present. As expected, these changes are not significant due to the unprecedented nature of the 2019 event.

Discussion

The analysis presented in this paper aimed to investigate the effectiveness of the MoSE system in reducing the damages caused by Acqua Alta events in Venice. To achieve

this goal, the study used an empirical approach to estimate the relationship between sea level and economic damages, and evaluated the effectiveness of the MoSE system in mitigating the damages caused by events similar to the three most devastating events in the past.

The results of the analysis show that, for events similar to the 1966 event, the MoSE system has already produced significant savings in terms of economic damages, compared to the counterfactual scenario where the MoSE system was not in place. For the 2018 event, there is a balance of cost/benefit but only one analogue event that caused the MoSE activation has been observed so far. Finally, the results also highlights the limitations of the analysis when MoSE system is used to mitigate the damages caused by unprecedented events, such as the 2019 events. This is due to the lack of analogues of such events in the near present and suggest that our analysis shall be repeated in the future when disposing of a larger sample of events similar to 2018 and 2019.

While our study provides important insights into the relationship between sea level and damages caused by Acqua Alta events in Venice, there are several limitations that should be considered when interpreting our results.

First, our analysis relies on identifying analogues based on the sea level pressure (SLP) field of the event, which may not fully capture all the relevant atmospheric and oceanic conditions that contribute to Acqua Alta. Moreover, our database of historical SLP fields is limited, and future studies may benefit from incorporating additional data sources and using more advanced machine learning techniques to improve the accuracy of the analogues identification process. Our analysis is based on empirical estimates of the relationship between sea level and damages, which may be subject to errors and biases. In particular, our model assumes a linear relationship between sea level and damages, which may not hold for extreme events or under changing climatic conditions. Furthermore, our data on damages is limited to reported losses, which may not capture the full extent of the economic and social impacts of Acqua Alta events. Finally, our analysis does not incorporate information from climate models or other types of climate projections, which could help to assess the potential impacts of future climate change on Acqua Alta events in Venice. Incorporating such information would require additional data sources and modeling techniques, and may be subject to uncertainties and biases associated with the models themselves. The use of large ensemble simulations will also help in discriminating the role of antrhopogenically driven changes of these patterns from the long term variability of the climate system.

In conclusion, the results of this study have important implications for the management of Acqua Alta events in Venice. While we cannot attribute the observed changes exclusively to one factor, the modifications of atmospheric circulation patterns due to both natural and anthropogenic forced variability leading to Acqua Alta events already greatly affect the city of Venice. Our findings suggest that the MoSE system can be an effective mitigation strategy for events with historical analogues, but additional measures may be needed to address the potential damages caused by unprecedented events. Future research in this area should focus on improving the accuracy of analogues identification, incorporating more sophisticated modeling techniques, and expanding the range of data sources and variables used to assess the impacts of

Acqua Alta events. From the point of view of impacts, future research should focus to better understand the effectiveness of the MoSE system in mitigating damages caused by Acqua Alta events and to identify additional measures that can be implemented to reduce the impacts of these events on the city of Venice.

Our study represents one of the first examples that goes beyond identifying the circulation drivers of extreme events to quantifying the changes and their impacts. The framework we presented is general and can be applied to other case studies. However, our study also has limitations, including the limited database of sea-level for the past, the limited analogues used, and the fact that we did not use climate models. Despite these limitations, our study provides important insights into the attribution and impacts of extreme events, which are crucial for developing effective mitigation and adaptation strategies. We hope that our work will inspire future research and inform policymakers in their efforts to reduce the risks associated with extreme events.

Methods

Data

We utilized the latest climate reanalysis data produced by the European Centre for Medium-Range Weather Forecasts (ECMWF) as part of the implementation of the EU-funded Copernicus Climate Change Service (C3S). Specifically, we used the ERA5 dataset, which provides hourly data on atmospheric, land surface, and sea state parameters from 1950 to the present at a horizontal resolution of $0.25°\times0.25°$ [27]. The choice of using ERA5 data for this study was motivated by the dataset's consistency over a long period of time (73 years), which allowed us to detect changes in the large dynamics associated with Acqua Alta events. Additionally, the global nature of the ERA5 dataset allowed us to avoid mixing data from different national weather services and ensured uniform spatial and temporal coverage. While other observational or reanalysis datasets were considered, such as E-OBS, MERRA, NCEP, and CFSR, these were discarded due to the lack of sea-point coverage or insufficient temporal and spatial resolutions. The Centro Previsioni e Segnalazioni Maree (Center for Tides Forecasting and Reporting) of the Venice Municipality provides tide gauge data that is essential for understanding the frequency and intensity of Acqua Alta events in Venice. The tide gauge data records the water levels in the Venetian Lagoon at 16 different locations, including the historical station of Punta della Salute. These measurements are taken every 1 hour and are reported in centimeters above the mean sea level, referred to the tidal zero of Punta della Salute. The tide level data are freely available at https://www.comune.venezia.it/it/content/dati-dalle-stazioni-rilevamento.

Analogues Methods

The attribution protocol described in Faranda et al. [25] has already been applied and validated for pressure maps leading up to series of extreme events in the year 2021, including floods in Westphalia [28], storm Alex [29], and wind-power changes [30].

Here we apply it for Acqua Alta events in Venice, as follows. The typical time scales of Acqua Alta events in Venice is two days so, before the analyse we perform a

grid-point by grid-point moving average of the atmospheric fields analysed in the day of the event and the day before the event. Results do not change significantly if instead of two days, we perform the moving average over three days. We divide the ERA5 sea-level pressure data set into two periods: 1950-1979 and 1993-2022 each consisting of 30 years of daily data. We consider the first period to represent a past world with a weaker anthropogenic influence on climate than the second period, which represents our factual world affected by anthropogenic climate change. Here, we assume that 30 years is a long enough period to average out high-frequency interannual variability of the atmospheric motions. This time period is also recommended by the WMO for the computation of climate normals [31].

To account for the possible influence of low-frequency modes of natural variability in explaining the differences between the two periods, we also consider the possible roles of the El Niño-Southern Oscillation (ENSO), the Atlantic Multidecadal Oscillation (AMO), and the Pacific Decadal Oscillation, the main sources of natural variability.

For each period, we examine all daily sea level pressure records and select the best 17 analogues, i.e. the records minimizing the Euclidean distance to the event record itself. The number of 17 corresponds approximately to the smallest 1‰ Euclidean distances in each subset of our data. We tested the extraction of 10 to 20 analogous records, without finding qualitatively important differences in our results. For the factual period, as is customary in attribution studies, the event itself is excluded. In addition, we prohibit the search for analogues within a one-week window centered on the date of the event. Finally, we examine the seasonality of the analogues during the relevant season and their association with ENSO, PDO and AMO. We perform this last analysis using monthly indices from NOAA/ERSSTv5 data and retrieved from the Royal Netherlands Meteorological Institute (KNMI) Climate Explorer. In particular, the ENSO index is version 3.4 as defined by Huang et al. [32], and the AMO, PDO index is calculated as described in Trenberth and Shea [33]. When the ENSO 3.4 index is positive, it corresponds to El Niño, and when it is negative, it corresponds to La Niña.

We define several quantities to support our interpretation of analogue-based assignment, including the analogue quality Q, which is the average Euclidean distance of a given day from its 17 closest analogues. If the value of Q for the extreme event belongs to the same distribution of its analogues, then the event is not unprecedented, and the attribution can be performed. If the value of Q is greater than those of its analogues, the event is unprecedented and not attributable.

We also use dynamical systems theory to compute the local dimension D of each SLP map, which is a proxy for the number of degrees of freedom of the field, and the persistence index Θ, which estimates the number of days we are likely to observe a map that is an analogue of the one under consideration. We compute the values of persistence for the extreme event in the past, factual and counterfactual world and the corresponding distributions of the persistence for the analogues.

We count the number of analogues in each month of the extended Autumn season (September, October, November, December) to detect whether there has been a shift

in circulation to months earlier or later in the season. This can have strong thermodynamic implications, for example, if a circulation leading to large positive temperature anomalies in early spring becomes more frequent later in the season when average temperatures are much higher.

Economic Damage Model vs. sea-level

We use an empirical approach to estimate the relation between sea level reached within the lagoon and economic damages to find an analytical function. We based our estimation on the reported damages associated with the three most devastating events (04/11/1966, 29/10/2018, and 12/11/2019) which were 8000 MEUR, 47 MEUR, and 1000 MEUR, respectively (https://www.businessinsider.com/flooding-cost-1-billion-of-damage-to-venice-tourist-attractions-2019-12?r=US&IR=T, https://www.bbc.co.uk/newsround/50902267). Damage estimates are adjusted by the inflation (http://resolver.tudelft.nl/uuid:ea34a719-79c1-4c6e-b886-e0d92407bc9d). According to previous employed models for estimating hazard functions for floods [34–37] we use an exponential law Damage$[MEUR] = a \exp b\, SL^*$, where $SL^* = SL/110$, to link the economic damage (in millions of euros) and the observed sea level change for extreme sea levels larger than 110 cm. The parameters of the fit are estimated by using the Levenberg-Marquardt algorithm whose robustness is assessed by the Least Absolute Residuals (LAR) method to minimize the absolute difference of the residuals. The best-fit parameters are $a = 5.05(3.06, 7.03) \times 10^{-3}$ MEUR and $b = 0.35(0.25, 0.45)$, where in brackets we report the 95% confidence levels, with an adjusted $R^2 = 0.99$ and a Root Mean Squared Error (RMSE = 27). We also used a power-law fit to model the economic damages as a function of the sea level, Damage$[MEUR] = a\, SL^{*b}$, with best-fit parameters $a = 8.97(4.07, 13.09) \times 10^{-3}$ MEUR and $b = 66.19(47.04, 85.34)$, where in brackets we report the 95% confidence levels, with an adjusted $R^2 = 0.84$ and RMSE = 46. However, the results are not statistically confident due to the under-estimation of damages for sea levels less than 160 cm. We are aware that only 3 events are not sufficient to provide a robust assessment of fitting procedures, however the use of exponential models to describe cost-benefit assessments and risk-hazard results has been widely documented in literature for different scenarios [34–36]. Furthermore, natural hazards are generally characterized by exponential laws in their occurrence as well as in their effects [38] or modeled as cascade processes (i.e., with a power-law model) where the resulting dynamics is a series of mutually interconnected phenomena (as in turbulence [39, 40]).

References

[1] Tebaldi, C., Ranasinghe, R., Vousdoukas, M., Rasmussen, D.J., Vega-Westhoff, B., Kirezci, E., Kopp, R.E., Sriver, R., Mentaschi, L.: Extreme sea levels at different global warming levels. Nature Climate Change **11**(9), 746–751 (2021) https://doi.org/10.1038/s41558-021-01127-1

[2] Umgiesser, G., Bajo, M., Ferrarin, C., Cucco, A., Lionello, P., Zanchettin, D., Papa, A., Tosoni, A., Ferla, M., Coraci, E., Morucci, S., Crosato, F., Bonometto, A., Valentini, A., Orlić, M., Haigh, I.D., Woge Nielsen, J., Bertin, X., Bustorff Fortunato, A., Pérez Gómez, B., Alvarez Fanjul, E., Paradis, D., Jourdan, D., Pasquet, A., Mourre, B., Tintoré, J., Nicholls, R.J.: The prediction of floods in Venice: methods, models and uncertainty (review article). Natural Hazards and Earth System Sciences **21**(8), 2679–2704 (2021) https://doi.org/10.5194/nhess-21-2679-2021

[3] Lionello, P., Barriopedro, D., Ferrarin, C., Nicholls, R.J., Orlić, M., Raicich, F., Reale, M., Umgiesser, G., Vousdoukas, M., Zanchettin, D.: Extreme floods of Venice: characteristics, dynamics, past and future evolution (review article). Natural Hazards and Earth System Sciences **21**(8), 2705–2731 (2021) https://doi.org/10.5194/nhess-21-2705-2021

[4] Zanchettin, D., Bruni, S., Raicich, F., Lionello, P., Adloff, F., Androsov, A., Antonioli, F., Artale, V., Carminati, E., Ferrarin, C., Fofonova, V., Nicholls, R.J., Rubinetti, S., Rubino, A., Sannino, G., Spada, G., Thiéblemont, R., Tsimplis, M., Umgiesser, G., Vignudelli, S., Wöppelmann, G., Zerbini, S.: Sea-level rise in Venice: historic and future trends (review article). Natural Hazards and Earth System Sciences **21**(8), 2643–2678 (2021) https://doi.org/10.5194/nhess-21-2643-2021

[5] Ferrarin, C., Lionello, P., Orlić, M., Raicich, F., Salvadori, G.: Venice as a paradigm of coastal flooding under multiple compound drivers. Scientific Reports **12**, 5754 (2022) https://doi.org/10.1038/s41598-022-09652-5

[6] Miglietta, M.M., Carnevale, D., Levizzani, V., Rotunno, R.: Role of moist and dry air advection in the development of Mediterranean tropical-like cyclones (medicanes). Quarterly Journal of the Royal Meteorological Society **147**(735), 876–899 (2021) https://doi.org/10.1002/qj.3951

[7] Luppichini, M., Bini, M., Barsanti, M., Giannecchini, R., Zanchetta, G.: Seasonal rainfall trends of a key Mediterranean area in relation to large-scale atmospheric circulation: How does current global change affect the rainfall regime? Journal of Hydrology **612**, 128233 (2022) https://doi.org/10.1016/j.jhydrol.2022.128233

[8] Flaounas, E., Davolio, S., Raveh-Rubin, S., Pantillon, F., Marcello Miglietta, M., Gaertner, M.A., Hatzaki, M., Homar, V., Khodayar, S., Korres, G., Kotroni, V., Kushta, J., Reale, M., Ricard, D.: Mediterranean cyclones: current knowledge and open questions on dynamics, prediction, climatology and impacts. Weather and Climate Dynamics **3**(1), 173–208 (2022) https://doi.org/10.5194/wcd-3-173-2022

[9] Davolio, S., Silvestro, F., Gastaldo, T.: Impact of Rainfall Assimilation on High-Resolution Hydrometeorological Forecasts over Liguria, Italy. Journal of Hydrometeorology **18**(10), 2659–2680 (2017) https://doi.org/10.1175/JHM-D-17-0073.1

[10] Davolio, S., Miglietta, M.M., Diomede, T., Marsigli, C., Montani, A.: A flood episode in northern Italy: multi-model and single-model mesoscale meteorological ensembles for hydrological predictions. Hydrology and Earth System Sciences **17**(6), 2107–2120 (2013) https://doi.org/10.5194/hess-17-2107-2013

[11] Otto, F.E.L.: Extreme events: The art of attribution. Nature Climate Change **6**(4), 342–343 (2016) https://doi.org/10.1038/nclimate2971

[12] Otto, F.: Attribution of extreme weather events: how does climate change affect weather? Weather **74**(9), 325–326 (2019) https://doi.org/10.1002/wea.3610

[13] IPCC: Climate Change 2022: Mitigation of Climate Change. Contribution of Working Group III to the Sixth Assessment Report of the Intergovernmental Panel on Climate Change. Cambridge University Press, Cambridge, UK and New York, NY, USA (2022). https://doi.org/10.1017/9781009157926

[14] Van Oldenborgh, G.J., Wehner, M.F., Vautard, R., Otto, F.E.L., Seneviratne, S.I., Stott, P.A., Hegerl, G.C., Philip, S.Y., Kew, S.F.: Attributing and Projecting Heatwaves Is Hard: We Can Do Better. Earth's Future **10**(6), 2021–002271 (2022) https://doi.org/10.1029/2021EF002271

[15] Vautard, R., Kadygrov, N., Iles, C., Boberg, F., Buonomo, E., Bülow, K., Coppola, E., Corre, L., van Meijgaard, E., Nogherotto, R., Sandstad, M., Schwingshackl, C., Somot, S., Aalbers, E., Christensen, O.B., Ciarlo, J.M., Demory, M.-E., Giorgi, F., Jacob, D., Jones, R.G., Keuler, K., Kjellström, E., Lenderink, G., Levavasseur, G., Nikulin, G., Sillmann, J., Solidoro, C., Sørland, S.L., Steger, C., Teichmann, C., Warrach-Sagi, K., Wulfmeyer, V.: Evaluation of the Large EURO-CORDEX Regional Climate Model Ensemble. Journal of Geophysical Research (Atmospheres) **126**(17), 2019–032344 (2021) https://doi.org/10.1029/2019JD032344

[16] van Oldenborgh, G.J., van der Wiel, K., Kew, S., Philip, S., Otto, F., Vautard, R., King, A., Lott, F., Arrighi, J., Singh, R., van Aalst, M.: Pathways and pitfalls in extreme event attribution. Climatic Change **166**(1-2), 13 (2021) https://doi.org/10.1007/s10584-021-03071-7

[17] Reed, K.A., Wehner, M.F., Zarzycki, C.M.: Attribution of 2020 hurricane season extreme rainfall to human-induced climate change. Nature Communications **13**, 1905 (2022) https://doi.org/10.1038/s41467-022-29379-1

[18] Bellprat, O., Guemas, V., Doblas-Reyes, F., Donat, M.G.: Towards reliable extreme weather and climate event attribution. Nature Communications **10**, 1732 (2019) https://doi.org/10.1038/s41467-019-09729-2

[19] Strauss, B.H., Orton, P.M., Bittermann, K., Buchanan, M.K., Gilford, D.M., Kopp, R.E., Kulp, S., Massey, C., Moel, H.d., Vinogradov, S.: Economic damages

from Hurricane Sandy attributable to sea level rise caused by anthropogenic climate change. Nature Communications **12**, 2720 (2021) https://doi.org/10.1038/s41467-021-22838-1

[20] Ranasinghe, R., Ruane, A.C., Vautard, R., Arnell, N., Coppola, E., Cruz, F.A., Dessai, S., Islam, A.S., Rahimi, M., Ruiz Carrascal, D., Sillmann, J., Sylla, M.B., Tebaldi, C., Wang, W., Zaaboul, R.: Climate Change Information for Regional Impact and for Risk Assessment. In Climate Change 2021: The Physical Science Basis. Contribution of Working Group I to the Sixth Assessment Report of the Intergovernmental Panel on Climate Change. Cambridge University Press, Cambridge, UK and New York, NY, USA (2021). https://doi.org/10.1017/9781009157896.014

[21] Sperotto, A., Torresan, S., Gallina, V., Coppola, E., Critto, A., Marcomini, A.: A multi-disciplinary approach to evaluate pluvial floods risk under changing climate: The case study of the municipality of Venice (Italy). Science of the Total Environment **562**, 1031–1043 (2016) https://doi.org/10.1016/j.scitotenv.2016.03.150

[22] Leonardi, N.: The barriers of Venice. Nature Geoscience **14**(12), 881–882 (2021) https://doi.org/10.1038/s41561-021-00864-4

[23] Mel, R., Carniello, L., D'Alpaos, L.: Addressing the effect of the Mo.S.E. barriers closure on wind setup within the Venice lagoon. Estuarine Coastal and Shelf Science **225**, 106249 (2019) https://doi.org/10.1016/j.ecss.2019.106249

[24] Umgiesser, G., Matticchio, B.: Simulating the mobile barrier (MOSE) operation in the Venice Lagoon, Italy: global sea level rise and its implication for navigation. Ocean Dynamics **56**(3-4), 320–332 (2006) https://doi.org/10.1007/s10236-006-0071-4

[25] Faranda, D., Pascale, S., Bulut, B.: Persistent anticyclonic conditions and climate change exacerbated the exceptional 2022 European-Mediterranean drought. Environmental Research Letters **18**(3), 034030 (2023) https://doi.org/10.1088/1748-9326/acbc37

[26] Anderson, T.W.: On the distribution of the two-sample cramer-von mises criterion. The Annals of Mathematical Statistics, 1148–1159 (1962)

[27] Hersbach, H., Bell, B., Berrisford, P., Biavati, G., Horányi, A., Muñoz Sabater, J., Nicolas, J., Peubey, C., Radu, R., Rozum, I., et al.: ERA5 hourly data on single levels from 1959 to present. Copernicus Climate Change Service (C3S) Climate Data Store (CDS). (Accessed on 09-11-2022) (2018). https://doi.org/10.24381/cds.adbb2d47

[28] Faranda, D., Bourdin, S., Ginesta, M., Krouma, M., Noyelle, R., Pons, F., Yiou, P., Messori, G.: A climate-change attribution retrospective of some impactful

462 weather extremes of 2021. Weather and Climate Dynamics **3**(4), 1311–1340 (2022)
463 https://doi.org/10.5194/wcd-3-1311-2022

464 [29] Ginesta, M., Yiou, P., Messori, G., Faranda, D.: A methodology for attributing
465 severe extratropical cyclones to climate change based on reanalysis data: the case
466 study of storm Alex 2020. Climate Dynamics (2022) https://doi.org/10.1007/
467 s00382-022-06565-x

468 [30] Rapella, L., Faranda, D., Gaetani, M., Drobinski, P., Ginesta, M.: Climate change
469 on extreme winds already affects off-shore wind power availability in europe.
470 Environmental Research Letters **18**(3), 034040 (2023) https://doi.org/10.1088/
471 1748-9326/acbdb2

472 [31] Arguez, A., Vose, R.S.: The Definition of the Standard WMO Climate Normal:
473 The Key to Deriving Alternative Climate Normals. Bulletin of the Amer-
474 ican Meteorological Society **92**(6), 699–704 (2011) https://doi.org/10.1175/
475 2010BAMS2955.1

476 [32] Huang, B., Shin, C.-S., Shukla, J., Marx, L., Balmaseda, M.A., Halder, S.,
477 Dirmeyer, P., Kinter, I. James L.: Reforecasting the ENSO Events in the Past 57
478 Years (1958-2014). Journal of Climate **30**(19), 7669–7693 (2017) https://doi.org/
479 10.1175/JCLI-D-16-0642.1

480 [33] Trenberth, K.E., Shea, D.J.: Atlantic hurricanes and natural variability in
481 2005. Geophys. Res. Lett. **33**(12), 12704 (2006) https://doi.org/10.1029/
482 2006GL026894

483 [34] Amadio, M., Scorzini, A.R., Carisi, F., Essenfelder, A.H., Domeneghetti, A.,
484 Mysiak, J., Castellarin, A.: Testing empirical and synthetic flood damage mod-
485 els: the case of italy. Natural Hazards and Earth System Sciences **19**(3), 661–678
486 (2019) https://doi.org/10.5194/nhess-19-661-2019

487 [35] Gerl, T., Kreibich, H., Franco, G., Marechal, D., Schröter, K.: A review of flood
488 loss models as basis for harmonization and benchmarking. PLOS ONE **11**(7),
489 1–22 (2016) https://doi.org/10.1371/journal.pone.0159791

490 [36] Read, L.K., Vogel, R.M.: Hazard function analysis for flood
491 planning under nonstationarity. Water Resources Research
492 **52**(5), 4116–4131 (2016) https://doi.org/10.1002/2015WR018370
493 https://agupubs.onlinelibrary.wiley.com/doi/pdf/10.1002/2015WR018370

494 [37] Guan, X., Xia, C., Xu, H., Liang, Q., Ma, C., Xu, S.: Flood risk analysis
495 integrating of bayesian-based time-varying model and expected annual dam-
496 age considering non-stationarity and uncertainty in the coastal city. Journal of
497 Hydrology **617**, 129038 (2023) https://doi.org/10.1016/j.jhydrol.2022.129038

[38] Read, L.K., Vogel, R.M.: Hazard function theory for nonstationary natural hazards. Natural Hazards and Earth System Sciences **16**(4), 915–925 (2016) https://doi.org/10.5194/nhess-16-915-2016

[39] Frisch, U., Sornette, D.: Extreme Deviations and Applications. Journal de Physique I **7**(9), 1155–1171 (1997) https://doi.org/10.1051/jp1:1997114 arXiv:cond-mat/9705132 [cond-mat.stat-mech]

[40] Alberti, T., Daviaud, F., Donner, R.V., Dubrulle, B., Faranda, D., Lucarini, V.: Chameleon attractors in turbulent flows. Chaos Solitons and Fractals **168**, 113195 (2023) https://doi.org/10.1016/j.chaos.2023.113195

Data Availability

ERA5 data are publicly available at climate explorer (http://climexp.knmi.nl/). Sea level data are made available at https://www.comune.venezia.it/it/content/centro-previsioni-e-segnalazioni-maree from the Centro Previsione e Segnalazione Maree - Protezione Civile, Venice, Italy, under the License Creative Commons Attribution-NonCommercial-ShareAlike 3.0 Italy (CC BY-NC-SA 3.0 IT).

Code Availability

The code to perform the analogues dynamical analysis is available at https://fr.mathworks.com/matlabcentral/fileexchange/95768-attractor-local-dimension-and-local-persistence-computation.

Acknowledgments

All the authors acknowledge the Centro Previsione e Segnalazione Maree - Protezione Civile, Venice, Italy, for making available tide gauge data. Data are distributed under the License Creative Commons Attribution-NonCommercial-ShareAlike 3.0 Italy (CC BY-NC-SA 3.0 IT). DF and EC received support from the European Union's Horizon 2020 research and innovation programme under grant agreement No. 101003469 (XAIDA). DF received further support from the European Union's Horizon 2020 Marie Sklodowska-Curie grant agreement No. 956396 (EDIPI) and the LEFE-MANU-INSU-CNRS grant "CROIRE".

Author Contributions

DF and TA devised the study, DF performed the analogues analyses and TA devised the model of damage. All authors contributed to discussing and writing the paper.

Competing Interest

The authors declare no competing interests nor conflicts of interest. No human or animal data have been used in this study.

Declarations

The authors declare no conflict of interests.

Supplementary Information for: Attributing Venice Acqua Alta events to a changing climate and evaluating the efficacy of MoSE adaptation strategy

Davide Faranda[1,2,3*], Tommaso Alberti[4], Erika Coppola[5], Marco Anzidei[4]

[1*]Laboratoire des Sciences du Climat et de l'Environnement, CEA Saclay l'Orme des Merisiers, UMR 8212 CEA-CNRS-UVSQ, Gif-sur-Yvette, 91191, France.
[2]London Mathematical Laboratory, 8 Margravine Gardens, London, W6 8RH, UK.
[3]Laboratoire de Météorologie Dynamique/IPSL, École Normale Supérieure, PSL Research University, Sorbonne Université, 75005, Paris, France, École Polytechnique, IP Paris, Paris, 75005, France.
[4]Istituto Nazionale di Geofisica e Vulcanologia, via di Vigna Murata 605, Rome, 00143, Italy.
[5]International Centre for Theoretical Physics, Strada Costiera 11, Trieste, 34100, Italy.

*Corresponding author(s). E-mail(s): davide.faranda@lsce.ipsl.fr;
Contributing authors: tommaso.alberti@ingv.it; coppolae@ictp.it; marco.anzidei@ingv.it;

Abstract

The supplementary material of this paper provides additional detailed analyses of the extreme flooding events that occurred in Venice in 1966, 2018 and 2019. The material includes detailed methodological element, explanation and figures that show the temporal evolution of sea-level pressures, temperatures, precipitations, wind speed of the three events analysed Additionally, the material provides detailed information on the sea-level and the estimated damages caused by the

flooding, including the affected area for 2018 and 2019. The supplementary material also includes a comparison between the 2018 and 2019 events with the 1966 Great Flood of Venice, highlighting similarities and differences in terms of sea level, storm surge, and damage.

Keywords: Climate Change, Attribution, Sea Level, Adaptation

1 Supplementary Methods

1.1 Analogue quality Q

: Q is the average Euclidean distance of a given day from its 17 closest analogues. If the value of Q for the extreme event belongs to the same distribution of its analogues then the event is not unprecedented and the attribution can be performed, if the value of Q is greater than those of its analogues the event is unprecedented and therefore not attributable.

1.2 Predictability Index D

Using dynamical systems theory [1–3], we can compute the local dimension D of each slp map [4, 5]. The local dimension is a proxy for the number of degrees of freedom of the field, meaning that the higher D, the more unpredictable the temporal evolution of the slp maps will be [6–8]. If the dimension D of the derecho event analyzed is higher or lower than that of its analogues, then the extreme will be respectively less or more predictable than the closest dynamical situations identified in the data. The attractor of a dynamical system is a geometric object defined in the space hosting all the possible states of the system (phase-space). Each point ζ on the attractor can be characterized by two dynamical indicators: the local dimension D, which indicates the number of degrees of freedom active locally around ζ, and the persistence Θ, a measure of the mean residence time of the system around ζ [6, 9]. To determine D, we exploit recent results from the application of extreme value theory to Poincaré recurrences in dynamical systems. This approach considers long trajectories of a system — in our case successions of daily SLP latitude–longitude maps — corresponding to a sequence of states on the attractor. For a given point ζ in phase space (e.g., a given SLP map), we compute the probability that the system returns within a ball of radius ϵ centered on the point ζ. The Freitas et al. [10] theorem, modified by Lucarini et al. [11], states that logarithmic returns:

$$g(x(t)) = -\log(\mathrm{dist}(x(t), \zeta)) \tag{1}$$

yield a probability distribution such that:

$$\Pr(z > s(q)) \simeq \exp\left[-\vartheta(\zeta)\left(\frac{z-\mu(\zeta)}{\sigma(\zeta)}\right)\right] \tag{2}$$

where $z = g(x(t))$ and s is a high threshold associated to a quantile q of the series $g(x(t))$. Requiring that the orbit falls within a ball of radius ϵ around the point ζ is

equivalent to asking that the series $g(x(t))$ is over the threshold s; therefore, the ball radius ϵ is simply $e^{-s(q)}$. The resulting distribution is the exponential member of the Generalized Pareto Distribution family. The parameters μ and σ, namely the location and the scale parameter of the distribution, depend on the point ζ in phase space. $\mu(\zeta)$ corresponds to the threshold $s(q)$ while the local dimension $D(\zeta)$ can be obtained via the relation $\sigma = 1/D(\zeta)$. This is the metric of predictability introduced in Section **??**.

When $x(t)$ contains all the variables of the system, the estimation of D based on extreme value theory has a number of advantages over traditional methods (e.g. the box counting algorithm [12, 13]). First, it does not require to estimate the volume of different sets in scale-space: the selection of $s(q)$ based on the quantile provides a selection of different scales s which depends on the recurrence rate around the point ζ. Moreover, it does not require the a priori selection of the maximum embedding dimension as the observable g is always a univariate time-series.

1.3 Persistence Index Θ

The persistence of the state ζ is measured via the extremal index $0 < \vartheta(\zeta) < 1$, an dimensionless parameter, from which we extract $\Theta(\zeta) = \Delta t/\vartheta(\zeta)$. Here, Δt is the timestep of the dataset being analysed. $\Theta(\zeta)$ is therefore the average residence time of trajectories around ζ, namely the metric of persistence introduced in Section **??**, and it has unit of a time (in this study days). If ζ is a fixed point of the attractor, then $\Theta(\zeta) = \infty$. For a trajectory that leaves the neighborhood of ζ at the next time iteration, $\Theta = 1$. To estimate ϑ, we adopt the Süveges estimator [14]. For further details on the the extremal index, see Moloney et al. [15].

2 Supplementary Analyses

2.1 Additional Analyses for the 1966 event

The quality of the analogues (Figure S1a) shows that this circulation is very uncommon compared to the rest of the analogues with no significant changes in the two periods. We detect visible changes in increase in predictability D (Figure S1b) while persistence Θ is the same in present and past periods (Figure S1c). The seasonal occurrence of analogues (Figure S1d) shows a shift towards the month of December in the present period. This explain why we do not observe a warming signal in Figure S2; The changes in ENSO (Figure S1e) are not statistically significant while AMO and PDO distributions have a significant shift between the two periods (Figure S1f) and g), suggesting a possible role of the inter-decadal variability of the Pacific and Atlantic Circulation in the occurrence of these events. Finally, when computing analogues for the whole period and counting their frequency per decade, we observe a non-significant increase, leading to about one more event each decade (Figure S1h).

2.2 Analyses for the 2018 event

On Monday, October 29, 2018, at 2:40 pm, the tide reached a value of 156cm in Punta Salute, Venice, causing significant flooding (https://www.comune.venezia.it/it/content/le-acque-alte-eccezionali#29ottobre). The event was partly caused by an

Atlantic disturbance that remained stable between the Gulf of Lyon and the Gulf of Genoa, but the effects were amplified by two blocking anticyclones positioned in Eastern Europe and the Azores [16]. The anticyclones caused a strong acceleration of the southerly winds along the Adriatic coast. On Monday, the atmospheric pressure in Venice dropped by 12 hPa in 16 hours. The southerly wind had been blowing since Sunday, reaching an average speed of around 60km/h and gusts of up to 95km/h. The wind blew violently in the lagoon, especially when a convective thunderstorm generated over Venice in the evening. The intense gusts raised internal waves in the main canals of the city and islands, causing significant damage to the barriers, including those protecting the tide center, residential buildings, and commercial activities. The flooding covered 73% of the pedestrian areas and ranked fourth in importance, equaled with the level reached on December 1, 2008. The lowest level was 119cm at 5:35 pm, the highest in history, except for the 1966 event, which registered 116cm. In the evening, the maximum was 148cm at 8:25 pm, ranking seventh in height and covering about 65% of the Venice's walkable surface. The consecutive presence of the sea level above 120cm was approximately 14 hours, equaling the 1966 record.

Figure S2 shows the results of the attribution of the synoptic configuration associated with the episode. The domain analyzed is 2°E-17°W 36°N-51°N. The slp field of the event (Figure S2a) has been used for the search of 17 analogues for the past and present periods. Their average is displayed respectively in Figure S3b,c). We observe significant differences in the pressure field when subtracting present from past analogues leading to more anticyclonic conditions in the present (Figure S2d). The atmospheric pattern of the present period is further associated with higher temperatures over some Mediterranean region (Figure S2e-h) and higher precipitation over Veneto and Friuli possibly enhancing the impact of these events compared to the past (Figure S2i-l). Winds (Figure S2m-p) are generally stronger on the Thyrrenian sea but not on the Adriatic. The quality of the analogues (Figure S2q) shows that this circulation is relatively rare compared to the rest of the analogues with no significant changes in the two periods. Q for the events remain in the bulk of the distribution of analogs quality for the past period but it is at the edge of the distribution for the present period so that the slp pattern examined is not highlighted as dynamically unprecedented by this analysis. We do not detect visible changes in predictability D (Figure S2r) nor on the persistence Θ (Figure S2s) relative to the past world by half of the day. The seasonal occurrence of analogues (Figure S2t) does not present any significantly shifts from past to present period. The changes in ENSO (Figure S2u) are not statistically significant while AMO and PDO distributions have a significant shift between the two periods (Figure S2v,w), suggesting a possible role of the interdecadal variability of the Pacific and Atlantic Circulation in the occurrence of these patterns. Finally, when computing analogues for the whole period and counting their frequency per decade, we observe a non-significant decrease of events, leading to about one less event each decade (Figure S2x).

2.3 Analyses for the 2019 event

To understand the causes of the Aqua Granda phenomenon that occurred on November 12th, we needed to reconstruct the meteorological situation of that day, which

developed within the framework of the particular meteorological situation of the entire month (https://www.comune.venezia.it/it/content/le-acque-alte-eccezionali#12novembre2019). We have come to the conclusion that the exceptional levels of high tide recorded on November 12, 2019, cannot be attributed solely to the Sirocco wind blowing in the Adriatic Sea [16, 17]. A comparison with the Vaia storm that occurred on October 29, 2018, shows that although the meteorological contribution in 2018 was much greater, the maximum contribution occurred during a minimum astronomical tide. On the other hand, in the case of the unfortunate coincidence of November 12th, 2019, the peak of the meteorological contribution coincided perfectly with the peak of the astronomical tide [16, 18].

Moreover, the strength of the local wind was also unusual, due to an exceptional meteorological situation [16, 19]. Our detailed analysis of the dynamics of atmospheric circulation can help to understand what happened on the evening of November 12th. From November 11th to 12th, the movement of the depression center towards the southern Tyrrhenian Sea induced Sirocco winds along the Adriatic, but limited to the central basin. Persistent winds from the north, northeast with average speeds of up to 14 m/s were present in the northern Adriatic. On November 12, the movement towards the northeast of the main pressure minimum present over the Tyrrhenian Sea caused the formation of a secondary minimum on the Adriatic, downwind of the Umbro-Marchigiano Apennines. This is an event similar, on a smaller scale, to the much more common formation of a cyclone on the Gulf of Genoa as a result of the interaction between a low pressure system coming from the west and the Alpine relief (the so-called "Alpine cyclogenesis"): a meteorological phenomenon extremely rare in the Upper Adriatic, both in terms of spatial and temporal dimensions, and with an equally unusual evolution. In the afternoon, this local depression moved northwestward to the Upper Adriatic, generating a reinforcement of winds from the Bora and Sirocco during its ascent from Marche to Veneto.

Figure S3 shows the results of the attribution of the synoptic configuration associated with the 2019 episode. The domain analyzed is 3°W-22°W 36°N-51°N. The slp field of the event (Figure S3a) has been used for the search of 17 analogues for the counterfactual and factual periods. Their average is displayed respectively in Figure S3b,c). We observe significant differences in the pressure field when subtracting present from past analogues leading to more anticyclonic conditions in the present (Figure S3d). The atmospheric pattern of the present period is further associated with higher temperatures over Africa (Figure S3e-h) and lower precipitation over the Mediterranean basin (Figure S3i-l). Winds (Figure S3m-p) are generally weaker on the Adriatic and the Jonian sea. The quality of the analogues (Figure S3q) shows that this circulation is extremely rare, compared to the rest of the analogues with no significant changes in the two periods. The pattern of 2019 event is therefore unprecedented. We do not detect visible changes in predictability D (Figure S3r) nor on the persistence Θ (Figure S3s) relative to the counterfactual world by half of the day. The seasonal occurrence of analogues (Figure S3t) does not present any significant shifts from past to present period. The changes in ENSO (Figure S3u) are statistically significant while for AMO changes are the limit of statistical significance and PDO distributions have a significant shift between the two periods (Figure S3v,w), suggesting a possible role of the

inter-decadal variability of the Pacific and Atlantic Circulation in the occurrence of these patterns. Finally, when computing analogues for the whole period and counting their frequency per decade, we observe a non-significant decrease of events, leading to about one/two less event each decade (Figure S3x).

References

[1] Freitas, A.C.M., Freitas, J.M., Todd, M.: Extreme value laws in dynamical systems for non-smooth observations. Journal of Statistical Physics **142**(1), 108–126 (2011)

[2] Freitas, A.C.M., Freitas, J.M., Vaienti, S.: Extreme Value Laws for sequences of intermittent maps. arXiv preprint arXiv:1605.06287 (2016)

[3] Lucarini, V., Faranda, D., Freitas, A.C.M., Freitas, J.M., Holland, M., Kuna, T., Nicol, M., Todd, M., Vaienti, S.: Extremes and Recurrence in Dynamical Systems. John Wiley & Sons, ??? (2016)

[4] Faranda, D., Messori, G., Alvarez-Castro, M.C., Yiou, P.: Dynamical properties and extremes of Northern Hemisphere climate fields over the past 60 years. Nonlinear Processes in Geophysics **24**(4), 713–725 (2017)

[5] Faranda, D., Messori, G., Vannitsem, S.: Attractor dimension of time-averaged climate observables: insights from a low-order ocean-atmosphere model. Tellus A: Dynamic Meteorology and Oceanography **71**(1), 1–11 (2019)

[6] Faranda, D., Messori, G., Yiou, P.: Dynamical proxies of north atlantic predictability and extremes. Scientific reports **7**, 41278 (2017)

[7] Messori, G., Caballero, R., Faranda, D.: A dynamical systems approach to studying midlatitude weather extremes. Geophysical Research Letters **44**(7), 3346–3354 (2017)

[8] Hochman, A., Alpert, P., Harpaz, T., Saaroni, H., Messori, G.: A new dynamical systems perspective on atmospheric predictability: Eastern mediterranean weather regimes as a case study. Science advances **5**(6), 0936 (2019)

[9] Alberti, T., Faranda, D., Lucarini, V., Donner, R.V., Dubrulle, B., Daviaud, F.: Scale dependence of fractal dimension in deterministic and stochastic Lorenz-63 systems. Chaos **33**(2), 023144 (2023) https://doi.org/10.1063/5.0106053 arXiv:2206.13154 [nlin.CD]

[10] Freitas, A.C.M., Freitas, J.M., Todd, M.: Hitting time statistics and extreme value theory. Probability Theory and Related Fields **147**(3-4), 675–710 (2010)

[11] Lucarini, V., Faranda, D., Wouters, J.: Universal behaviour of extreme value statistics for selected observables of dynamical systems. Journal of statistical

physics **147**(1), 63–73 (2012)

[12] Liebovitch, L.S., Toth, T.: A fast algorithm to determine fractal dimensions by box counting. physics Letters A **141**(8-9), 386–390 (1989)

[13] Sarkar, N., Chaudhuri, B.B.: An efficient differential box-counting approach to compute fractal dimension of image. IEEE Transactions on systems, man, and cybernetics **24**(1), 115–120 (1994)

[14] Süveges, M.: Likelihood estimation of the extremal index. Extremes **10**(1-2), 41–55 (2007)

[15] Moloney, N.R., Faranda, D., Sato, Y.: An overview of the extremal index. Chaos: An Interdisciplinary Journal of Nonlinear Science **29**(2), 022101 (2019)

[16] Ferrarin, C., Bajo, M., Benetazzo, A., Cavaleri, L., Chiggiato, J., Davison, S., Davolio, S., Lionello, P., Orlić, M., Umgiesser, G.: Local and large-scale controls of the exceptional Venice floods of November 2019. Progress in Oceanography **197**, 102628 (2021) https://doi.org/10.1016/j.pocean.2021.102628

[17] Umgiesser, G., Bajo, M., Ferrarin, C., Cucco, A., Lionello, P., Zanchettin, D., Papa, A., Tosoni, A., Ferla, M., Coraci, E., Morucci, S., Crosato, F., Bonometto, A., Valentini, A., Orlić, M., Haigh, I.D., Woge Nielsen, J., Bertin, X., Bustorff Fortunato, A., Pérez Gómez, B., Alvarez Fanjul, E., Paradis, D., Jourdan, D., Pasquet, A., Mourre, B., Tintoré, J., Nicholls, R.J.: The prediction of floods in Venice: methods, models and uncertainty (review article). Natural Hazards and Earth System Sciences **21**(8), 2679–2704 (2021) https://doi.org/10.5194/nhess-21-2679-2021

[18] Lionello, P., Barriopedro, D., Ferrarin, C., Nicholls, R.J., Orlić, M., Raicich, F., Reale, M., Umgiesser, G., Vousdoukas, M., Zanchettin, D.: Extreme floods of Venice: characteristics, dynamics, past and future evolution (review article). Natural Hazards and Earth System Sciences **21**(8), 2705–2731 (2021) https://doi.org/10.5194/nhess-21-2705-2021

[19] Conte, D., Tiesi, A., Cheng, W., Papa, A., Miglietta, M.M.: Nowcasting of wind in the venice lagoon using wrf-fdda. Atmosphere **14**(3) (2023) https://doi.org/10.3390/atmos14030502

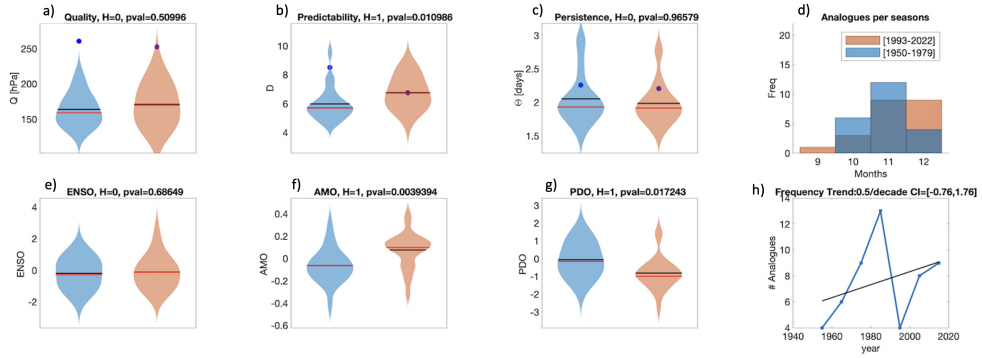

Fig. S1 Analogues Analysis for the 2018 Acqua Alta event in Venice. Violin plots for past (blue) and present (orange) periods for the analogues Quality Q (a) the Predictability index D (b), the Persistence index Θ (c) and the distribution of analogues in each month (d). Violin plots for past (blue) and present (orange) periods for ENSO (e), AMO (f), PDO (g). In the violin plots, red (black) lines represent average (median) values. The number of analogues per decade (blue) and its linear trend (black) in (h). Values for the peak day of the extreme event are marked by a dot. Titles in (a-h) report the results of the Cramer-von Mises test H and the pvalue pval. Title in panel (h) includes the value of the linear trend slope and its confidence interval CI in square brackets.

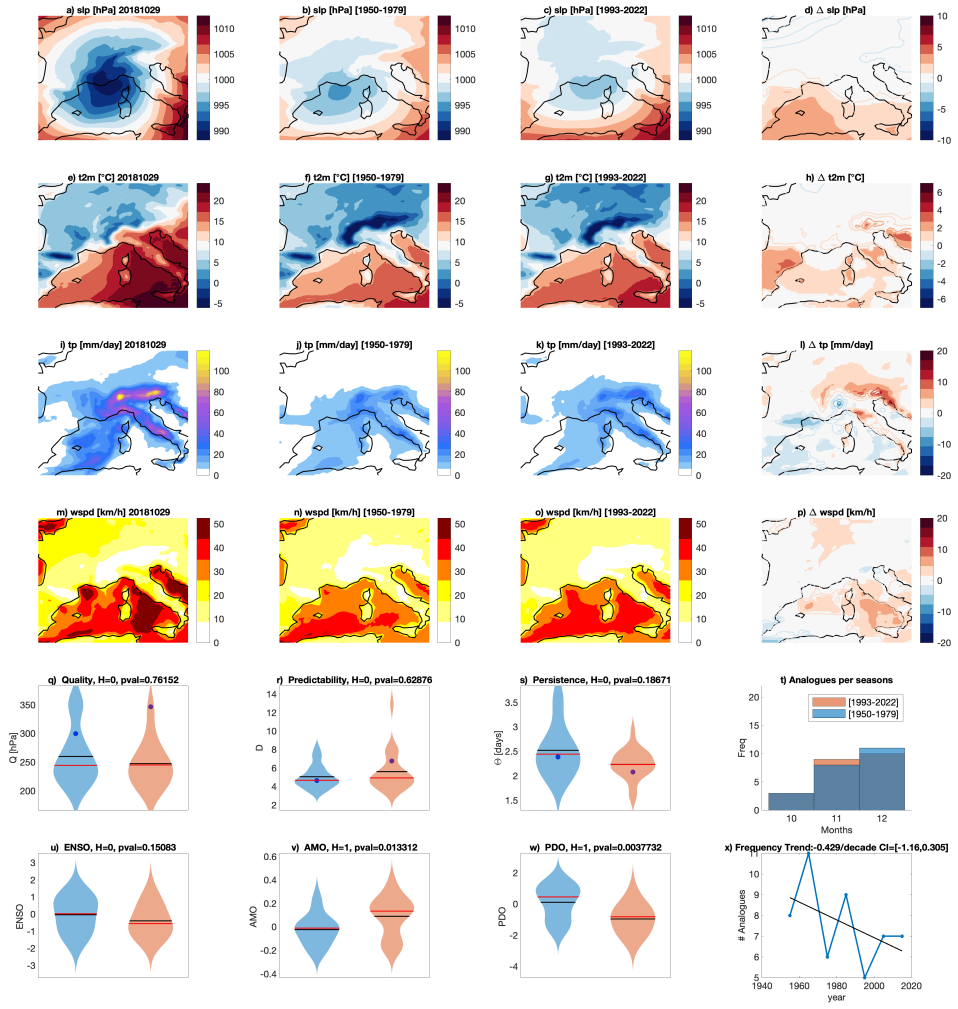

Fig. S2 Analogues Analysis for the 29/10/2018 Acqua Alta event in Venice. Daily mean sea-level pressure slp (a), 2-meter temperatures t2m (e), total precipitation tp (i), wind-speed wspd (m) on the day of the event. Average of the 17 sea-level pressure analogues found for the past [1950-1979] (b) and present [1993-2022] (c) periods and corresponding 2-meter temperatures (f,g), daily precipitation rate (j,k) and wind speed (n,o). Δslp (d), Δt2m (h), Δtp (i) and Δwspd (p) between present and past periods: colored-filled areas show significant anomalies with respect to the bootstrap procedure. Violin plots for past (blue) and present (orange) periods for the analogues Quality Q (q) the Predictability index D (r), the Persistence index Θ (s) and the distribution of analogues in each month (t). Violin plots for past (blue) and present (orange) periods for ENSO (u), AMO (v), PDO (w). The number of analogues per decade (blue) and its linear trend (black) in (x). Values for the peak day of the extreme event are marked by a dot. Titles in (q–v) report the results of the Cramer-von Mises test H and the pvalue pval. Title in panel (w) includes the value of the linear trend slope and its confidence interval CI in square brackets.

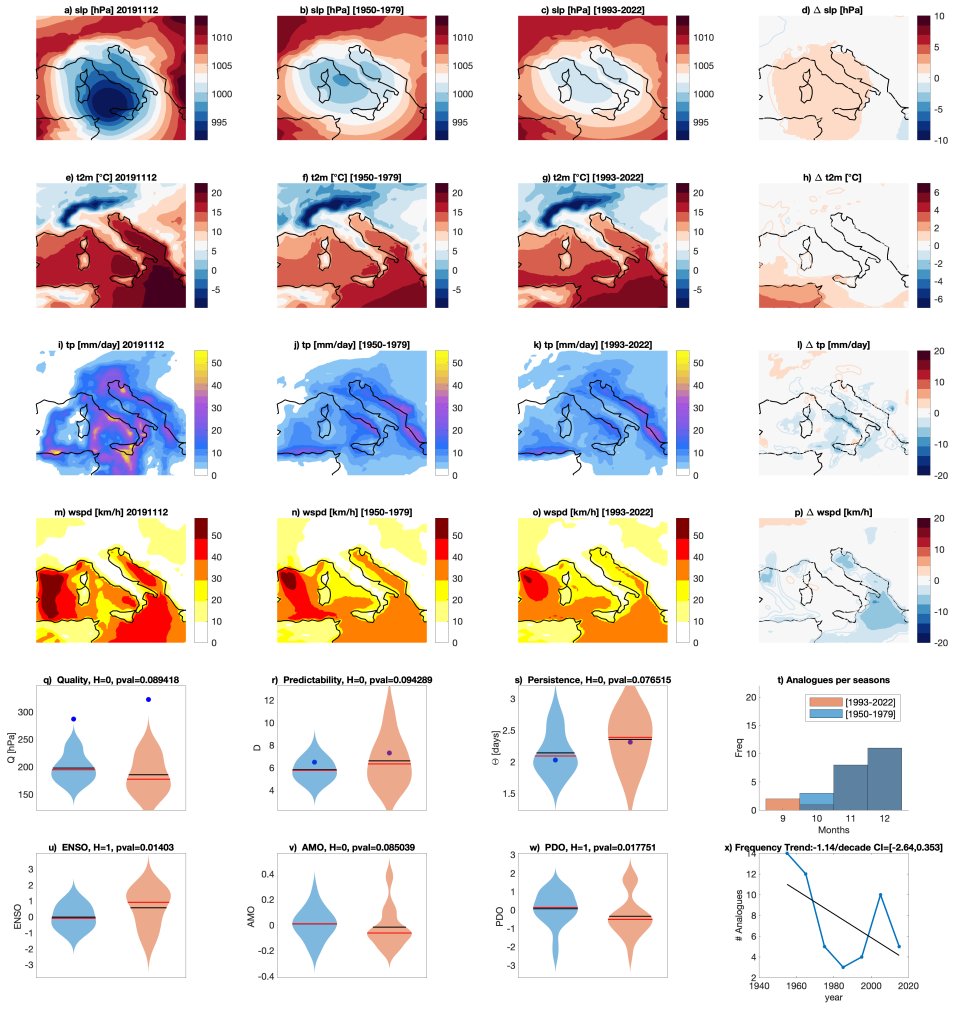

Fig. S3 Analogues Analysis for the 12/11/2019 Acqua Alta event in Venice. Daily mean sea-level pressure slp (a), 2-meter temperatures t2m (e), total precipitation tp (i), wind-speed wspd (m) on the day of the event. Average of the 17 sea-level pressure analogues found for the past [1950-1979] (b) and present [1993-2022] (c) periods and corresponding 2-meter temperatures (f,g), daily precipitation rate (j,k) and wind speed (n,o). Δslp (d), Δt2m (h), Δtp (i) and Δwspd (p) between past and present periods: colored-filled areas show significant anomalies with respect to the bootstrap procedure. Violin plots for past (blue) and present (orange) periods for the analogues Quality Q (q) the Predictability index D (r), the Persistence index Θ (s) and the distribution of analogues in each month (t). Violin plots for past (blue) and present (orange) periods for ENSO (u), AMO (v), PDO (w). The number of analogues per decade (blue) and its linear trend (black) in (x). Values for the peak day of the extreme event are marked by a dot. Titles in (q–v) report the results of the Cramer-von Mises test H and the pvalue pval. Title in panel (w) includes the value of the linear trend slope and its confidence interval CI in square brackets.

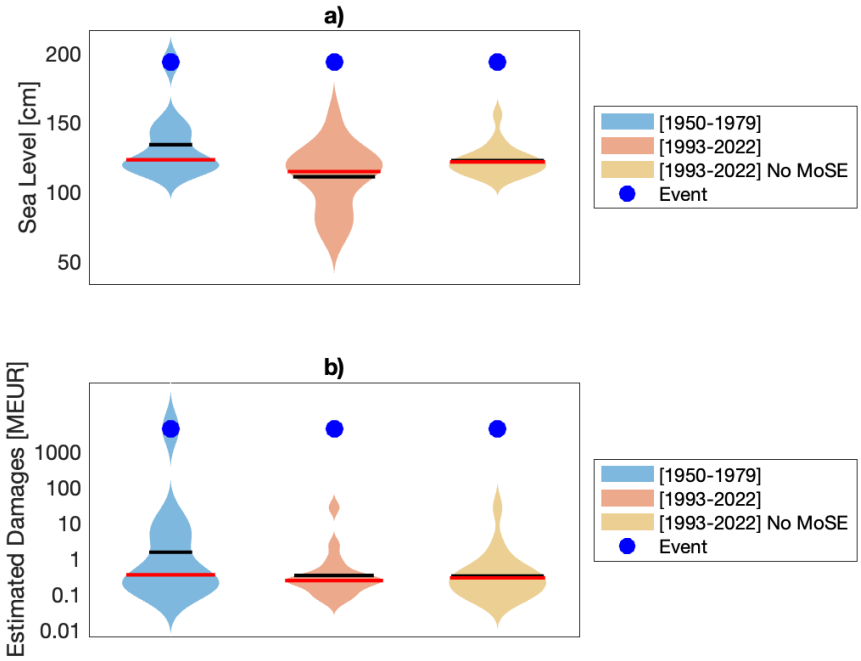

Fig. S4 Sea-levels SL during the analogues of the Acqua Alta 1966 event for past (blue), present (orange) and counterfactual worlds without MoSE (ocre) (a), and estimated damages of the flooding events associated (b). In the violin plots, red (black) lines represent average (median) values.

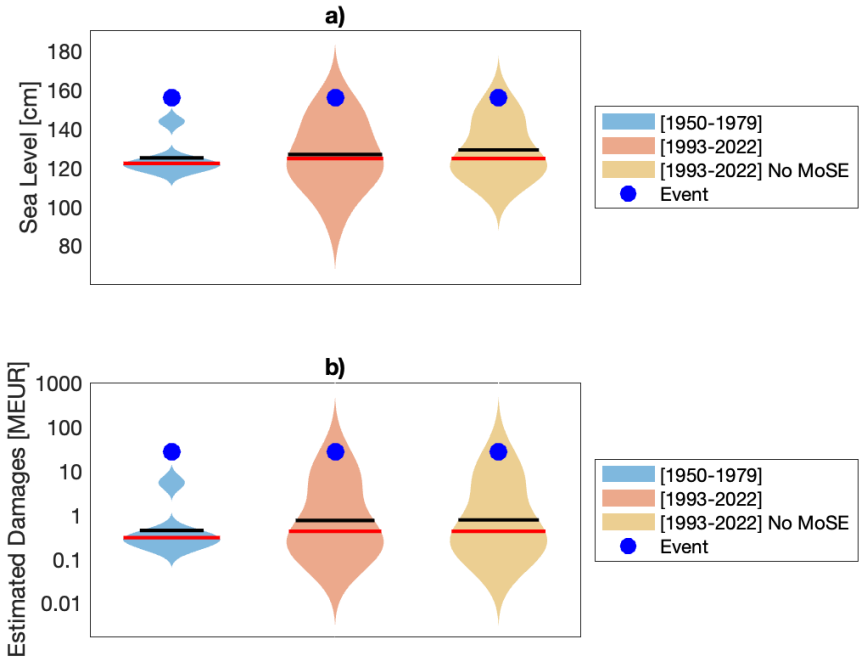

Fig. S5 Sea-levels SL during the analogues of the Acqua Alta 2018 event for past (blue), present (orange) and counterfactual worlds without MoSE (ocre) (a), and estimated damages of the flooding events associated (b). In the violin plots, red (black) lines represent average (median) values.

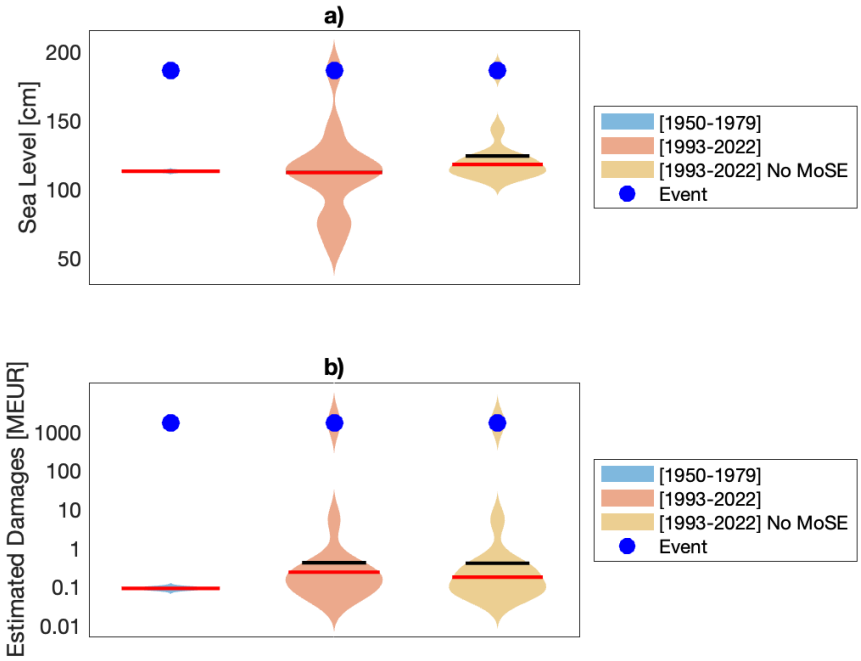

Fig. S6 Sea-levels SL during the analogues of the Acqua Alta 2019 event for past (blue), present (orange) and counterfactual worlds without MoSE (ocre) (a), and estimated damages of the flooding events associated (b).In the violin plots, red (black) lines represent average (median) values.